

# PERFORMANCE ANALYSIS OF A HIGHLY EFFICIENT DUAL OUTPUT BUCK CONVERTER WITH ZVS OPERATION FOR LED LIGHTING APPLICATIONS

S. Shameer<sup>1</sup> & Dr. D. Murali<sup>2</sup>

<sup>1</sup>Department of EEE, Government College of Engineering, Salem, Tamil Nadu, India, samir7vn@gmail.com

<sup>2</sup>Assistant Professor / EEE, Government College of Engineering, Salem, Tamil Nadu, India, muralid36@yahoo.com

**Abstract** – A very large number of LED (Light Emitting Diode) driver circuits with optimal design and high efficiency are being proposed in the literature in the recent past. However, only a few such designs are commercially successful because of the complexity involved in the design of control circuit and also the cost of the driver circuit is a key factor. This paper presents the design and analysis of a buck converter with dual output having less number of switching devices, along with brightness control for LED lamps. Majority of LED drivers need a conversion stage in case of AC input and a transformer for isolation which increase the cost of LED lamps. The proposed circuit is based on coupled inductor which acts as the energy transfer element and also eliminates the need for a transformer, thus providing the required isolation between the power circuit and low voltage LED circuit. Soft switching technique such as ZVS (Zero Voltage Switching) is employed to avoid voltage spikes during turn-off due to the leakage inductance of inductors. The brightness of the LEDs is controlled and regulated using double PWM (Pulse Width Modulation) method. The converter thus has high overall efficiency and better regulation compared to other single stage LED driver circuits. The proposed converter is simulated in PSIM 9.0 platform. The effectiveness of the proposed converter is validated through experimental results.

**Keywords:** LED, Double PWM, Lighting Load, Illumination, ZVS.

## 1. Introduction

Around 25% of the total electrical power demand globally is made up of lighting applications [1]. The contribution of solid-state devices in lighting has increased enormously over the past years due to the significant advantages they provide. Energy conservation has become more important than energy production [2]. LED lamps have found a huge market in residential, commercial and industrial lighting applications

because of its longevity, small size, durability and low power demand. When a LED driver utilizes an AC source as input, usually the conventional two-stage LED driver as shown in Fig. 1(a) is adopted. This two-stage structure is composed of power factor correction (PFC) regulator followed by a DC-DC converter. Thus, two-stage PFC technique needs more components, which increases converter size and control complexity significantly.

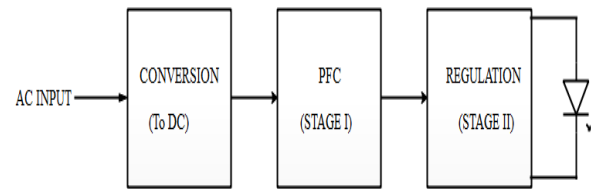


Fig. 1(a). Conventional Two-stage LED driver circuit

Fig. 1(b) shows the single-stage PFC circuit that provides both PFC operation and regulated DC voltage. A single DC-DC converter acts as both power factor correction circuit and also regulates the current output required to drive the LEDs.

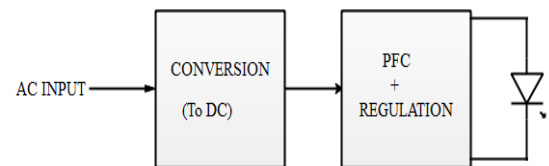


Fig. 1(b). Single-stage LED driver circuit

Many solutions for various problems are attained through research, but for any research to successfully transit as a commercial solution, cost of the solution plays a key role. The use of single-stage LED drivers are an attractive solution in

terms of cost and performance for LED lighting applications [3]. Due poor switch utilization of buck converter during low values of duty ratio, it becomes difficult to attain high step-down conversion ratio [4]. Circuit topologies employing coupled inductors (CI) have been proposed as an alternate solution for a conventional buck converter. The CI based topology can attain high step-down conversion ratio with increased duty ratio. The main problem with CI based topologies is the voltage spikes caused during turn-off due to the leakage inductance of the coupled inductors [5]. Many authors have proposed topologies with energy recycling of coupled inductors along with soft switching techniques to improve the efficiency and reduce switching losses. The Resonant Voltage Divider (RVD) technique is proposed in [6]. However, the major drawback of RVD topology is that it draws large surge currents at startup, which results in component failure.

Various soft switching converter topologies along with CI are presented in [7]-[11]. For high-power applications LEDs are connected in series, parallel and series-parallel strings. The problem with the series connection of LEDs is voltage balancing and also the damage of any one LED can cause failure of the entire string. Parallel connections require linear or switched regulators for current regulation, to balance the currents in the parallel paths. In [12], the hard switching step-down multi-output current auto-balancing LED driver is proposed, which has less efficiency and no illumination control.

The review of the proposed topologies suggests the need to develop a converter circuit with multiple outputs having a higher step-down ratio to achieve high efficiency [13]-[16]. Therefore, this work proposes a ZVS-Dual Output Coupled Inductor Buck converter to achieve high step-down voltage ratio, high power conversion efficiency, and with two different voltage levels. Dimming control of the multiple LEDs connected in parallel is studied. Regulation of average current flowing through the string is also discussed along with the design of the converter. Therefore, the proposed converter is an attractive choice for multi-output LED drivers with common input DC link or battery and only one switch per output with illumination control of each load. The main idea of proposed work is to achieve high efficiency of DC-DC post regulator as the second stage of conventional two-stage solution (PFC + post regulator). The proposed solution is cost-effective as compared with the three-stage solutions. The design analysis, considerations, and selection of switching devices are presented in section 2. The illumination control is discussed in section 3 followed by results and future enhancements in section 4. The experimental features of the proposed converter are given in section 5 and the conclusion is given in section 6.

## 2. Design Analysis of Proposed Converter

The proposed converter design is based on the integration of two converters. First one is the conventional buck converter and the second one is coupled inductor based buck converter.

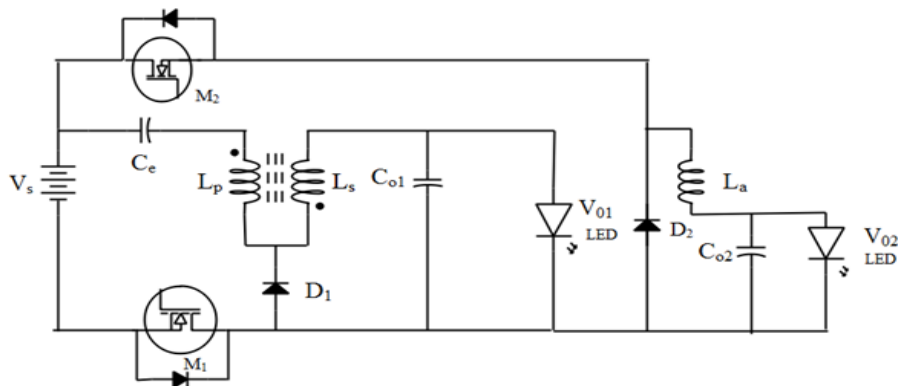


Fig. 2. Proposed Dual output Buck converter with ZVS.

The proposed converter design is shown in Fig. 2, which contains main switch ( $M_1$ ), auxiliary switch ( $M_2$ ), diodes ( $D_1$  &  $D_2$ ), and energy recycling capacitor ( $C_e$ ), primary inductance ( $L_p$ ) and secondary inductance ( $L_s$ ), auxiliary inductor ( $L_a$ ) and output capacitors ( $C_{o1}$  &  $C_{o2}$ ). Also, the input voltage / current is represented by  $V_{in} / i_{in}$ , the output voltage / current of load-1 is represented by  $V_{o1} / i_{o1}$ , and that of load-2 is represented by  $V_{o2} / i_{o2}$ . The equivalent representation of LED loads is denoted by  $R_{o1}$  and  $R_{o2}$ . The various circuit variables are defined as follows:  $i_{Lk}$  and  $V_{Lk}$  are leakage inductor current and voltage respectively,  $i_{Lp}$  and  $V_{Lp}$  are primary winding current and voltage respectively,  $i_{Ls}$  and  $V_{Ls}$  are secondary winding current and voltage respectively,  $i_{La}$  and  $V_{La}$  are auxiliary inductor current and voltage respectively,  $i_{D1}$  and  $V_{D1}$  are current and voltage of diode D1,  $i_{D2}$  and  $V_{D2}$  are current and voltage of diode D2.

#### A. Modes of operation

The operating principle of the proposed converter can be explained with the help of five different modes of operation. Each operating mode is illustrated with the help of equivalent circuits shown in Fig. 3.

1) Mode-1: This mode starts when main switch  $M_1$  is turned on. The diode  $D_1$  is in off state. The supply voltage is impressed over the combination of capacitor  $C_e$  and CI. Auxiliary switch  $M_2$  is in off state, but auxiliary inductor  $L_a$  is assumed to have charged in the previous cycle, therefore, it delivers power to load 2. The inductor leakage current is equal to the supply current during mode 1. The inductor currents slowly rise until the main switch is in ON state. This mode comes to an end when the main switch is turned off.

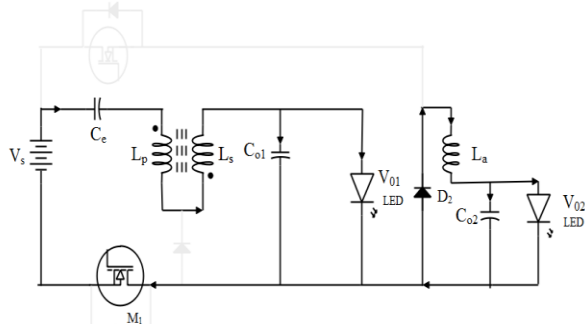


Fig. 3(a). Mode I equivalent circuit – primary inductor charging

2) Mode-2: During this mode, both the switches are in OFF state. This mode is also called energy transition mode since the stored energy in primary side  $L_p$  of coupled inductor is fed back through the body diodes of main switch  $M_1$  and auxiliary switches  $M_2$ . The diode  $D_1$  is conducting and secondary side  $L_s$  of CI powers load 1. The auxiliary inductor continues to power load 2. The junction capacitances of both the switches are charged and discharged in each cycle. In mode 2 the junction capacitance  $C_{M1}$  increases to voltage  $V_s$  from 0. At the same time, the junction capacitance of auxiliary switch  $C_{M2}$  becomes zero which leads to turn on of body diode.

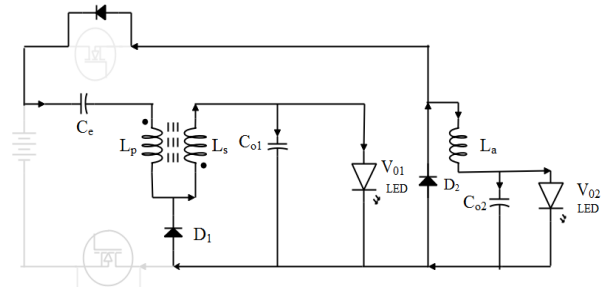


Fig. 3(b). Mode II equivalent circuit - transfer of stored energy in CI

3) Mode-3: In the previous mode, the body diode of  $M_2$  is conducting thus ensuring ZVS operation while the auxiliary switch is turned on. In this mode,  $L_a$  is completely demagnetized so diode  $D_2$  is turned off. The auxiliary inductor  $L_a$  is charged by the energy stored in the primary inductor during this mode and the current through the inductor rises linearly. Inductor  $L_s$  supplies load 1 in this mode. The charge stored in  $L_p$  is transferred back to supply via the junction capacitance  $C_{M1}$  of the main switch. The voltage across junction capacitance  $C_{M2}$  increases from 0 to  $V_s$ .

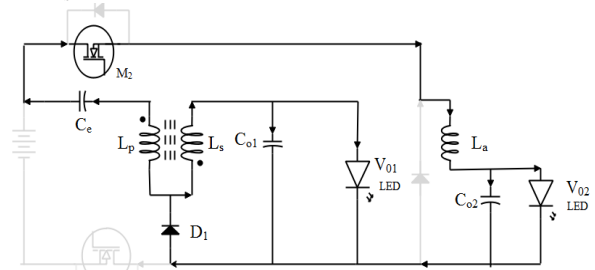


Fig. 3(c). Mode III equivalent circuit – Auxiliary inductor charging

4) Mode-4: The voltage across switch  $M_1$  becomes zero as the capacitance  $C_{M1}$  gets discharged completely. The body diode of switch  $M_1$  is turned on during this period. Both switches remain in off position and inductor  $L_s$  supplies load 1 and inductor  $L_a$  supplies load 2 respectively. The current through both the inductors is decreasing linearly. Since the energy stored in inductor  $L_p$  due to leakage current, is transferred back to supply via  $C_e$  the voltage spikes are reduced during turn off of the switches.

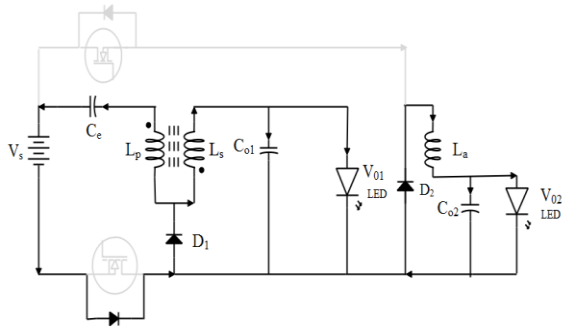


Fig. 3(d). Mode IV equivalent circuit – Recycling of stored energy

5) Mode-5: During this mode again the main switch  $M_1$  is turned on. Earlier, since the body diode of switch  $M_1$  is conducting it ensures that the voltage across the switch is zero and hence ZVS operation is achieved. The charge stored in primary inductor  $L_p$  is fed back to supply voltage  $V_s$  through switch  $M_1$ . The energy stored in auxiliary inductor  $L_a$  in the previous modes is used to supply load 2. At the end of the cycle diode,  $D_1$  gets reverse biased and the CI is charged again by input supply voltage, thus operation repeats in every cycle.

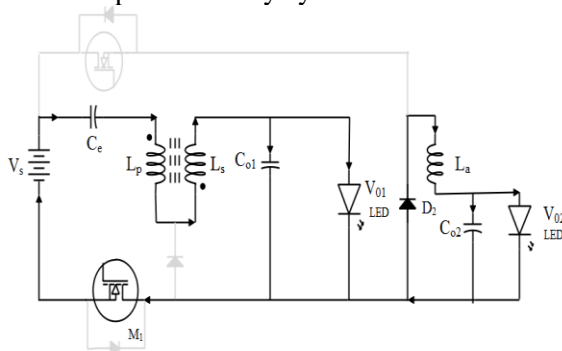


Fig. 3(e). Mode V equivalent circuit – Charging of Coupled Inductor

### 3. Illumination Control

The amount of flux or lumens required for a workplace greatly varies depending on the ambient conditions. Most of the lamps provide excess of lumens than required thus wasting power. Thus the control of illumination of LED lamps is done by dimming control circuits. Dimming control improves the comfort zone of humans in the working plane, it also increases the lifespan of LEDs by reducing the heat generated. The illumination of an LED light is roughly proportional to the average current flowing through it. By using amplitude modulation techniques and pulse width modulation techniques illumination can be varied [13]-[16]. The color spectrum of an LED depends on the current flowing through it, so that the color temperature of the LED lamp may vary with the current. By varying the duty ratio both amplitude modulation and PWM control can be achieved, but it leads to color discrepancy.

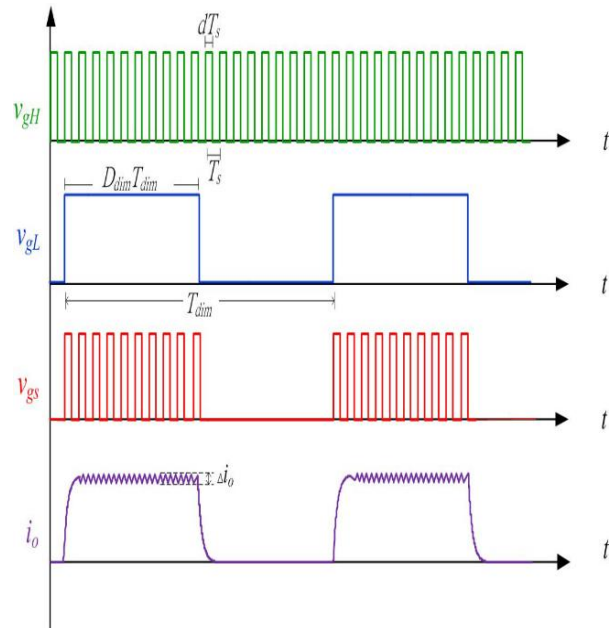


Fig. 4. Double PWM control scheme

Fig.4 illustrates the double PWM control scheme that is proposed to avoid this color shift in LED lights. The main switch  $M_1$  is gated by a PWM signal,  $V_{gL}$ , at a low frequency (dimming frequency) in association with a PWM signal,  $V_{gH}$ , at a high-frequency (switching frequency).

The dimming frequency is much lower than the switching frequency. The gating signal  $V_{gm}$  of  $M_1$  and  $V_{ga}$  of  $M_2$  is obtained from the “AND” result of  $V_{gL}$  and  $V_{gH}$ . The light output is proportional to the average current in LEDs. During the turn-on interval in each low-frequency dimming cycle, the magnitude of the pulsed current is regulated by PWM at the high switching frequency. Therefore, the average lamp current can be changed by adjusting the duty-ratios of either the low-frequency PWM or the high-frequency PWM.

#### 4. Simulation Results and Discussion

The simulation of the proposed converter is done using POWERSIM 9.0 software tool. The simulation circuit of the converter is shown in Fig. 5 and the parameters of the simulation circuit are listed in Table I.

Table I  
Simulation parameters for the proposed converter

Parameter	Value
$V_{in}$	125 V
$f_s$	100 KHz
$C_e$	1 $\mu$ F
$L_p$	1 mH
$L_s$	445 $\mu$ H
$L_a$	1.5 mH
$C_{01}$	800 $\mu$ F
$C_{02}$	60 $\mu$ F
$P_o$	16 W

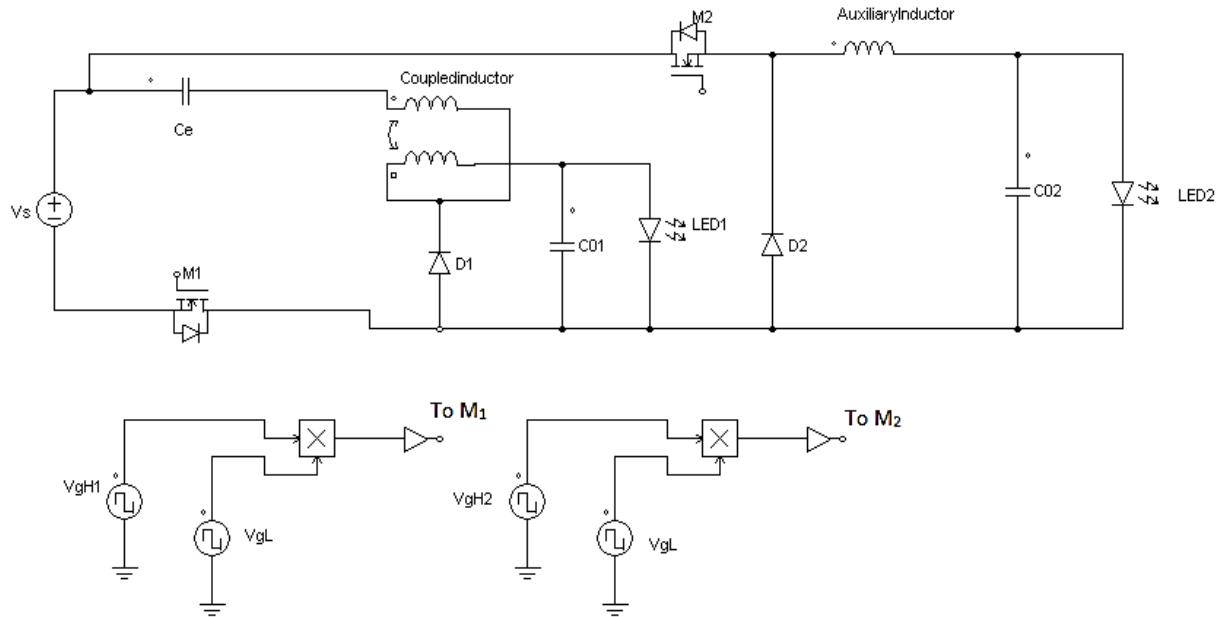


Fig. 5. Simulation circuit of proposed converter

The simulated waveforms for double PWM control strategy are shown in Fig. 6 where the high pulse is in the range of 100 KHz and low pulse is of 1000 Hz. The switching pulses for main switch  $M_1$  is obtained by comparing both the high and low pulses. The pulse signals for

switch  $M_2$  can be obtained by complementing the switching signals of  $M_1$  or it can be obtained by using a separate circuit as shown in Fig. 5. The output waveforms for 50% and 80% dimming are shown in Fig. 7. The ZVS operation of switches is illustrated in Fig. 8.

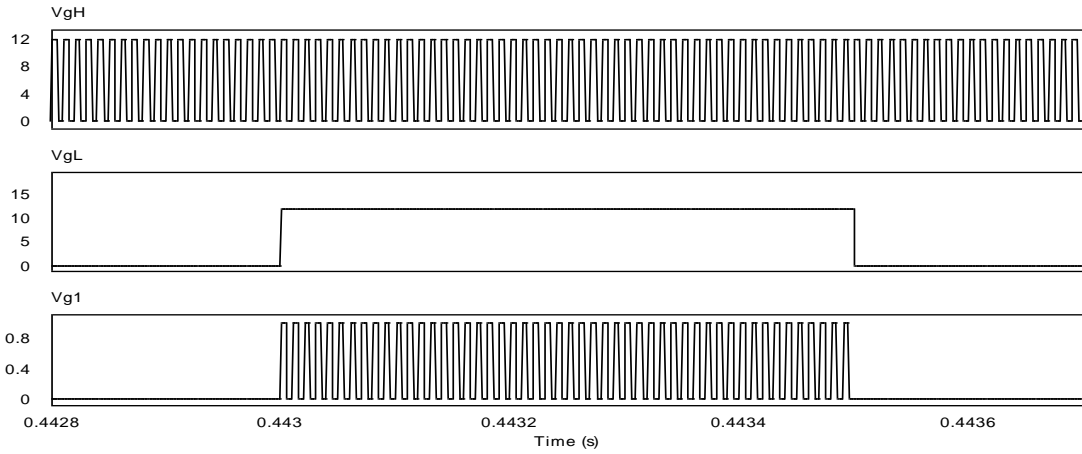


Fig. 6. Double PWM control strategy for generating switching pulses

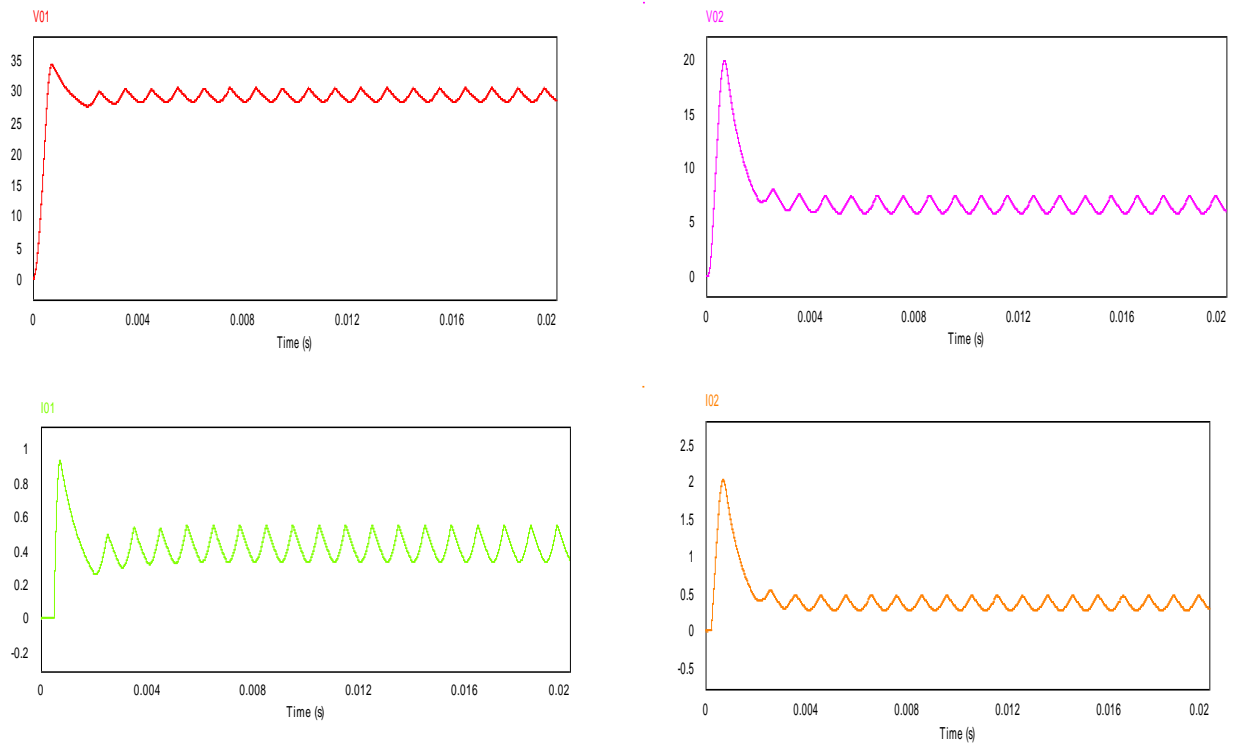


Fig. 7(a). Output waveforms for 50% dimming control

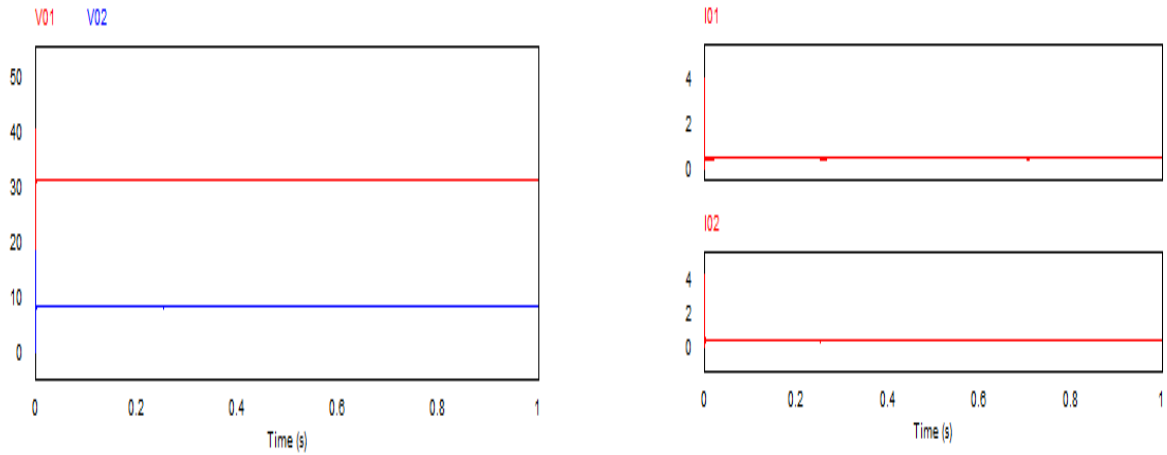


Fig. 7(b). Output waveforms for 100% dimming control

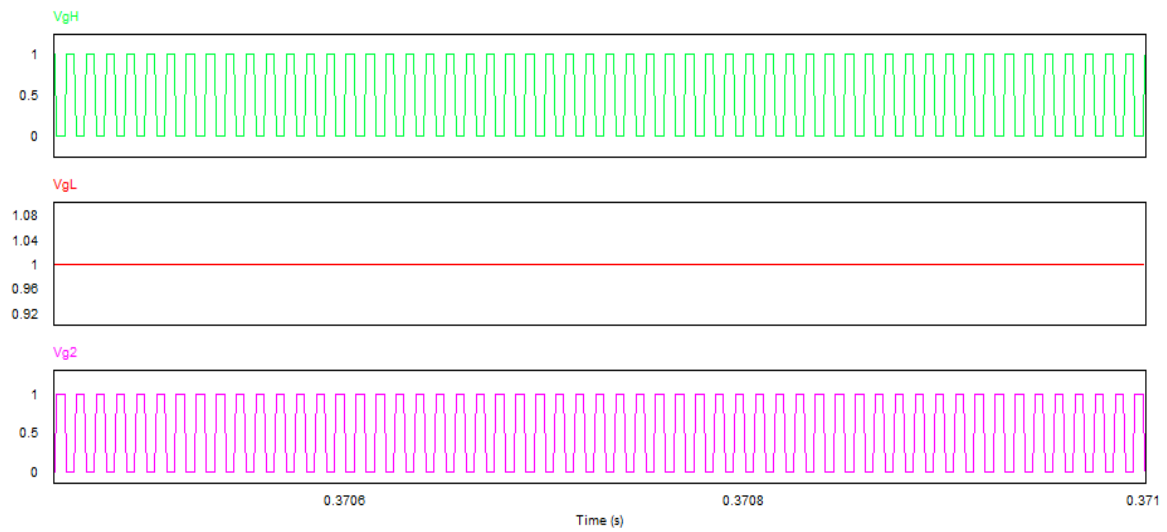


Fig. 7(c). Double PWM method for 100% dimming control

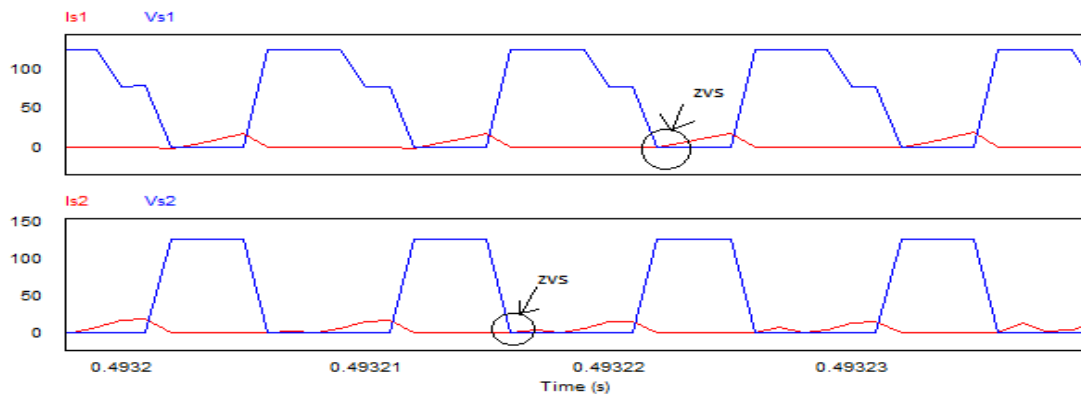


Fig. 8. Zero Voltage Switching operation waveforms for main and auxiliary switches



The performance of the proposed converter is analyzed with the help of efficiency and power factor at various modes of dimming control. At 100% dimming control the rated loads of 16W and 4W are achieved in the dual outputs of the converter respectively. At 50 % dimming, the power obtained is decreased. However, the

efficiency remains almost same and maintained around 95%. The efficiency of the proposed converter is compared with a hard switching converter proposed in [12]. The graph in Fig. 9 shows that the proposed converter is efficient for various load ranges than the converter in [12].

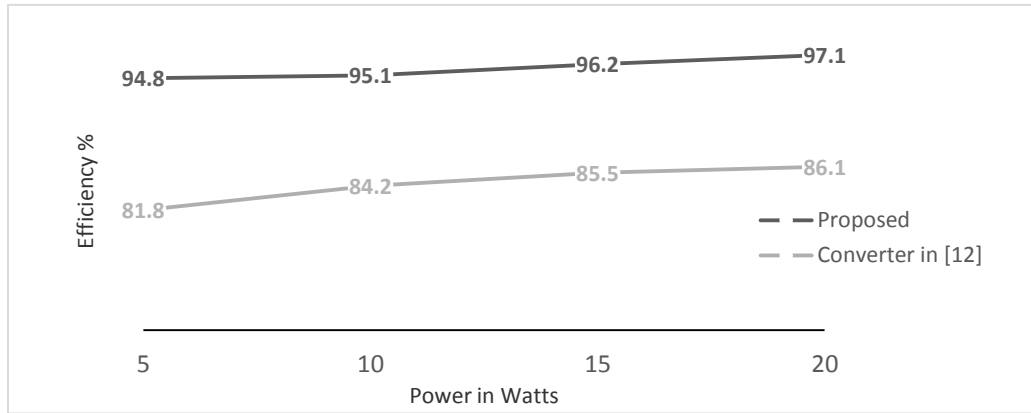


Fig. 9. Measured output efficiency Vs Load power rating

## 5. Experimental Results and Discussion

The proposed converter hardware implementation is carried out with two dual outputs having a voltage rating of 5V each with a current capability of 1 A. The total wattage rating of the prototype is 10W. The hardware circuit is implemented using a center tapped coupled inductor instead of using a coupled inductor and auxiliary inductor. The reason for using tapped arrangement is to reduce the size and overall dimension of the circuit and increase the efficiency. The gating pulses or the dimming control is achieved with the help of ATMEGA 328p micro-controller embedded in an ARDUINO-UNO launch kit. The program for double PWM control strategy is developed in ARDUINO IDE 1.8.1. The power supply for the converter is made of a center-tapped step-down transformer rated (15-0-15) V/ 3 A, followed by rectifier circuit made up of diodes 1N4007 and filter capacitor of 1000 $\mu$ F/ 25 V. The driver circuit used is push-pull driver circuit made up

of transistors BC139 and BC140. The switching device used is MOSFET IRF 540. The output stage consists of feedback diodes UF5408 and capacitors of rating 2200 $\mu$ F/ 50 V. The loads used are LEDs each of 5 V rating. The entire circuit diagram of the hardware implementation is shown in Fig.10. The hardware implementation differences have been made to test and analyze the performance of converter with the available input AC supply. The output voltage waveform of the hardware circuit is shown in Fig. 11. The port has been designed for a maximum output voltage of 5 V DC. The measured voltage drop across a single LED light is 2.2 V. Since the dual output ports have been designed for the same voltage rating, the voltage waveform for a single LED light load is presented as a slightly distorted waveform in Fig. 11. The double PWM high frequency and low frequency reference square waves are shown in Fig. 12(a) and Fig. 12(b).



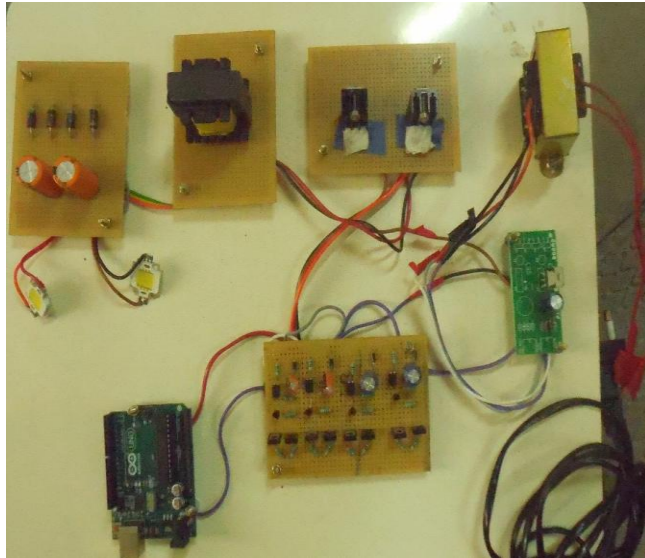


Fig. 10. Hardware implementation of LED driver with proposed converter

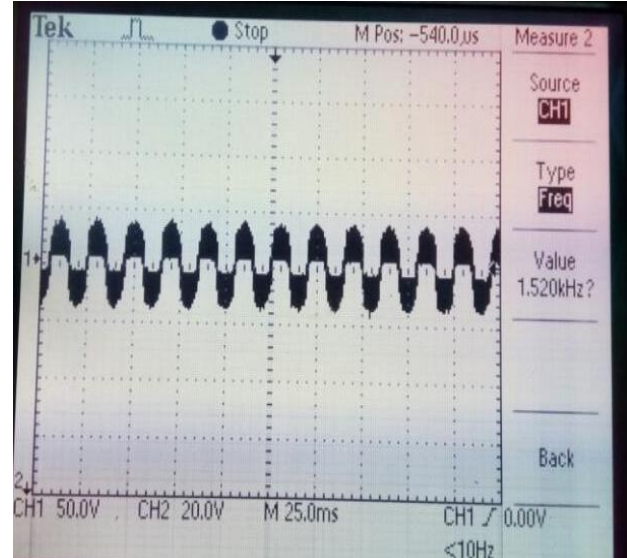


Fig. 12(a). Double PWM method -  $V_{gh}$  Low pulse

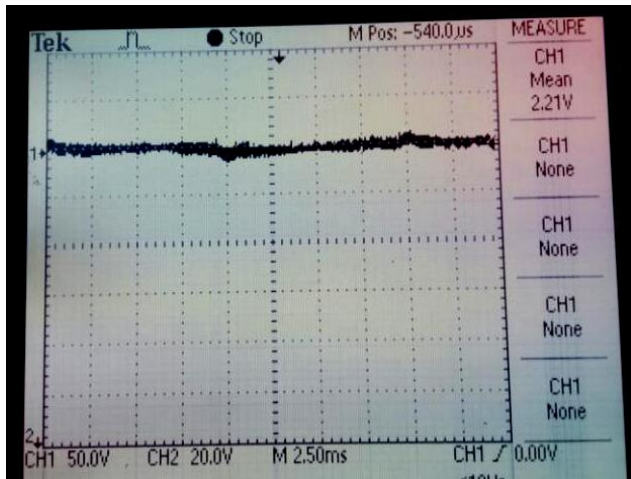


Fig. 11. Output voltage waveform across LED light

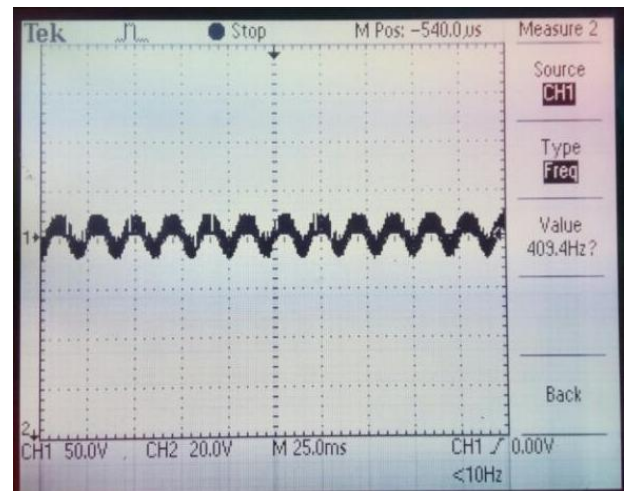


Fig. 12(b). Double PWM method -  $V_{gi}$  high pulse

## 6. Conclusion

This paper presents a modular and efficient buck converter design for driving LED lighting loads without color discrepancy. The number of output stages can be increased by adding an inductor as an auxiliary element along with a controlled switch. The requirement of power switches for each output stage is only one, thus reducing the cost and size of the converter. The additional advantage of the

converter is dimming control, which is achieved with help of double PWM control strategy that is used for both current regulation and power factor correction. The efficiency and effectiveness of the proposed LED driver are validated through hardware implementation.

## References

- [1] A. Lay-Ekuakille, F. D'Aniello, F. Miduri, D. Leonardi and A. Trotta, "Smart control of road-based LED fixtures for energy saving", *IEEE International Workshop on Intelligent Data Acquisition and Advanced Computing Systems: Technology and Applications*, Rende, 2009, pp. 59-62.
- [2] H. J. Chiu, Y. K. Lo, J. T. Chen, S. J. Cheng, C. Y. Lin and S. C. Mou, "A high-efficiency dimmable LED driver for low-power lighting applications", *IEEE Trans. on Ind. Electron.*, vol. 57, no. 2, pp. 735-743, Feb. 2010.
- [3] B. Singh, B. N. Singh, A. Chandra, K. Al-Haddad, A. Pandey and D. P. Kothari, "A review of single-phase improved power quality AC-DC converters", *IEEE Trans. on Ind. Electron.*, vol. 50, no. 5, pp. 962-981, Oct. 2003.
- [4] Kaiwei Yao, Mao Ye, Ming Xu and F. C. Lee, "Tapped-inductor buck converter for high-step-down DC-DC conversion", *IEEE Trans. on Power Electron.*, vol. 20, no. 4, pp. 775-780, July 2005.
- [5] B. L. Narasimharaju, S. P. Dubey and S. P. Singh, "Design and analysis of coupled inductor bidirectional DC-DC convertor for high-voltage diversity applications", *IET Power Electron.*, vol. 5, no. 7, pp. 998-1007, August 2012.
- [6] K. I. Hwu and Y. T. Yau, "Resonant voltage divider with bidirectional operation and startup considered", *IEEE Trans. on Power Electron.*, vol. 27, no. 4, pp. 1996-2006, April 2012.
- [7] S. S. Lee, "Step-down converter with efficient ZVS operation with load variation," *IEEE Trans. on Ind. Electron.*, vol. 61, no. 1, pp. 591-597, Jan. 2014.
- [8] H. L. Do, "Zero-Voltage-Switching synchronous buck converter with a coupled inductor", *IEEE Trans. on Ind. Electron.*, vol. 58, no. 8, pp. 3440-3447, Aug. 2011.
- [9] L. Jiang, C. C. Mi, S. Li, C. Yin and J. Li, "An improved soft-switching buck converter with coupled inductor", *IEEE Trans. on Power Electron.*, vol. 28, no. 11, pp. 4885-4891, Nov. 2013.
- [10] K. I. Hwu, W. Z. Jiang and Y. T. Yau, "Ultrahigh step-down converter", *IEEE Trans. on Power Electron.*, vol. 30, no. 6, pp. 3262-3274, June 2015.
- [11] K. I. Hwu, W. Z. Jiang and Y. T. Yau, "Nonisolated coupled-inductor based high step-down converter with zero DC magnetizing inductance current and nonpulsating output current", *IEEE Trans. on Power Electron.*, vol. 31, no. 6, pp. 4362-4377, June 2016.
- [12] Q. Luo, B. Zhu, W. Lu, and L. Zhou, "High step-down multiple-output LED driver with the current auto-balance characteristic", *Journal of Power Electronics*, vol. 12, no. 4, pp. 519-527, 2012.
- [13] Rong-Jong Wai and Rou-Yong Duan, "High step-up converter with coupled-inductor", *IEEE Trans. on Power Electronics*, vol. 20, no. 5, pp. 1025-1035, Sept. 2005.
- [14] K. H. Loo, W. K. Lun, S. C. Tan, Y. M. Lai, and C. K. Tse, "On driving techniques for LEDs: Toward a generalized methodology", *IEEE Trans. on Power Electron.*, vol. 24, no. 12, pp. 2967-2976, 2009.
- [15] K. H. Loo, Y. M. Lai, S. C. Tan and C. K. Tse, "On the color stability of Phosphor-converted white LEDs under DC, PWM, and bilevel drive", *IEEE Trans. on Power Electron.*, vol. 27, no. 2, pp. 974-984, Feb. 2012.
- [16] W. K. Lun, K. H. Loo, S. C. Tan, Y. M. Lai and C. K. Tse, "Bilevel current driving technique for LEDs", *IEEE Trans. on Power Electron.*, vol. 24, no. 12, pp. 2920-2932, Dec. 2009.